
Neural Attention Search

Difan Deng¹ Marius Lindauer^{1,2}

Abstract

We present Neural Attention Search (NAtS), a framework that automatically evaluates the importance of each token within a sequence and determines if the corresponding token can be dropped after several steps. This approach can efficiently reduce the KV cache sizes required by transformer-based models during inference and thus reduce inference costs. In this paper, we design a search space that contains three token types: (i) Global Tokens will be preserved and queried by all the following tokens. (ii) Local Tokens survive until the next global token appears. (iii) Sliding Window Tokens have an impact on the inference of a fixed size of the next following tokens. Similar to the One-Shot Neural Architecture Search approach, this token-type information can be learned jointly with the architecture weights via a learnable attention mask. Experiments on both training a new transformer from scratch and fine-tuning existing large language models show that NAtS can efficiently reduce the KV cache size required for the models while maintaining the models' performance.

1. Introduction

The ability to understand and infer from long-context information is crucial for many tasks such as long document summarization (Zhang et al., 2023a) and question answering (Kociský et al., 2018; Dasigi et al., 2021), code generation (Guo et al., 2023; Liu et al., 2024) or multi-round dialogues (Yi et al., 2024). Thanks to the ability to query the information from any position of the historical sequence, transformer-based large language models (Brown et al., 2020; Jiang et al., 2023; Anthropic, 2024; Grattafiori et al., 2024; Gemini & et al., 2024) extend their context length up to millions of tokens.

However, querying information from historical sequences

^{*}Equal contribution ¹Leibniz University Hannover ²L3S Research Center. Correspondence to: Difan Deng <d.deng@ai.uni-hannover.de>.

requires a complexity of $\mathcal{O}(L^2)$ w.r.t. the input sequence length L . KV caching could reduce this time complexity to $\mathcal{O}(L)$ by storing all the historical KV values. Nevertheless, with the increasing model size of recent LLMs, even the $\mathcal{O}(L)$ time-wise and memory-wise complexity could become a bottleneck during inference time.

Indeed, not all the tokens in a sequence are equally important. Many of them are redundant and do not contribute to the final output. Humans can recognize this information without pre-defined fixed rules and summarize or discard the context information into much smaller content. Transformers could also learn this ability implicitly: Many tokens in the attention map might only have very low weights (Zhang et al., 2023b) and only have little influence on the final predictions. However, as the transformer learns this information implicitly, we might not know how the important tokens would be distributed in the context. Selecting these tokens and recognizing the attention distributions might require extra human experts' knowledge by either looking at the attention maps (Liu et al., 2023; Zhang et al., 2023b; Feng et al., 2024; Zhang et al., 2024) or applying specific fixed rules (Child et al., 2019; Beltagy et al., 2024; Xiao et al., 2023; Chen et al., 2024; Ge et al., 2024). Since this knowledge is already contained in the transformer models, we could also ask the model to evaluate the importance of each token and learn to predict the optimal type for the given input tokens automatically.

Unlike prior works that rely on human expertise or pre-defined rules to identify important tokens, we propose a novel approach to evaluate the importance of each token by assigning different roles to each of the tokens. E.g. some tokens will be preserved until the end, while other tokens might only survive for a short amount of time. These roles measure the importance of each token and determine if they would survive within the next few tokens. Rather than pre-define a set of fixed rules for each token, we ask the model to learn this information automatically. Finding the optimal role for each token is similar to the process of neural architecture search (Elsken et al., 2019a; White et al., 2023), where an optimal architecture is searched by the optimizer for a given task. Thereby, in this work, we jointly optimize the choice of each token and the model weights by constructing a learnable attention mask. Our approach is implicitly motivated by the one-shot neural architecture search approach (Pham

et al., 2018; Liu et al., 2019; Dong & Yang, 2019), where the model parameter and architecture parameters are jointly optimized during the search process. However, our approach, Neural Attention Search (NATs), searches for the optimal token roles jointly with the attention weights.

Our contributions are as follows:

1. We propose Neural Attention Search (NATs), a framework that automatically searches for the optimal roles for each token in the input sequence.
2. We propose different token roles in our search space that can be later combined to construct a learnable attention mask and then jointly optimized with the model weights in NATs.
3. We show that NATs could efficiently reduce the KV cache required during inference time while maintaining most of the models’ performance.

By automatically learning to focus on the most relevant information, NATs paves the way for more efficient and scalable inference with LLMs in long-context applications.

2. Background and Related Work

2.1. Attention maps for transformers

Transformers (Vaswani et al., 2017) computes the correlation between different tokens by mapping the input sequences into three variables, Q , K and V . An attention map A is first computed by pairing Q and K and then scaled and normalized with a softmax function. Finally, this attention map A is multiplied by V . Additionally, a mask M is attached to the Attention Map to guide the attention to focus only on certain tokens. This can be expressed as

$$A = \frac{QK^T}{\sqrt{d_{head}}} \quad (1)$$

$$O = \text{softmax}(A + M^{add})V \quad (2)$$

The additive attention mask $M_{i,j}^{add} \in \{-\text{inf}, 0\}$ controls if the transformer needs to construct the correlation between Q_i and K_j . A widely used mask M^{add} used in transformers are casual masks (Vaswani et al., 2017), where the upper parts of the mask are filled with $-\text{inf}$ each token can only query the token information before them.

Computing the attention map of a sequence with length L requires a complexity of $\mathcal{O}(L^2)$ for both time and memory. Techniques such as KV cache lowers this complexity to the $\mathcal{O}(L_{cache})$ during inference time with L_{cache} being the length of the KV cache. However, as an expense, the cost of storing the KV cache gradually becomes unneglectable with the increasing size of large language models and the context length they could handle.

Many studies aim to reduce the KV cache size by sparsify-

ing the attention map with pre-defined rules. For instance, Sparse Attention (Child et al., 2019) combines the local sliding windows and trous attention to approximate the full attention maps; Longformer (Beltagy et al., 2024) further proposes to predefine a set of special tokens as global attention that have full access to any other tokens and can be queried by any other tokens; Streaming LLM (Xiao et al., 2023) shows that by preserving the initial tokens and the most recent tokens during inference time could recover the performance of window attention. DuoAttention (Xiao et al., 2024) further illustrates that only a small fraction of the attention heads are critical for processing long context information and therefore, only those retrieval heads should be preserved with the full attention. LongCoder (Guo et al., 2023) pre-defines a set of bridge tokens to summarize the information in between and memory tokens that will not be dropped afterwards. SepLLM (Chen et al., 2024) shows that the information contained in a segment can be compressed into a set of special tokens.

Alternatively, past attention maps can decide which tokens to evict or preserve. H2O (Zhang et al., 2023b) and Scissorhand (Liu et al., 2023) both identify the importance of each token based on their contributions to the attention maps and only preserve the most important tokens. Other approaches such as FastGen (Ge et al., 2024), SnapKV (Li et al., 2024), PyramidKV (Cai et al., 2024), and AadaKV (Feng et al., 2024) all applied pre-defined fixed rules to identify the important KV values. Additionally, instead of simply removing the unimportant tokens, we can also merge them into the existing tokens. CAM (Zhang et al., 2024) achieves this by merging the to-be-evicted tokens into the remaining tokens.

In contrast to the fine-tuning-free approaches above, alternatively, we can also fine-tune the target model to achieve the desired sparsity. Kim et al. (2022) ask the model to learn to drop the tokens with lower attention scores. Anagnostidis et al. (2023) shows that this sparsity can also be learned through sparse sigmoid functions. SPARSEK (Lou et al., 2024) only selects a constant number of KV Paris for each query by introducing a differentiable SparseK operator. Landmark Attention (Mohtashami & Jaggi, 2023) insert landmark tokens after certain time steps and apply these landmark tokens to summarize the information of the tokens before that landmark token and recover. Furthermore, Dynamic Token Pooling (Nawrot et al., 2023) segments the input sequences as pooling layers to reduce the overall computational costs, while Dynamic Memory Compression (Nawrot et al., 2024) tries to accumulate the tokens within the same subsequence into one single token.

While these existing methods offer various ways to reduce KV cache size, they often rely on inflexible predefined rules and potentially inaccurate heuristics based on past attention maps. NATs, in contrast, introduces a novel approach that

learns to dynamically assign token roles during inference, enabling a more adaptive and efficient use of the KV cache. By treating token role assignment as an optimization problem, NATS leverages principles from neural architecture search to jointly optimize token roles and model weights, leading to a more flexible and powerful attention mechanism.

2.2. Neural Architecture Search

Designing a neural architecture for a specific task might require a lot of trial and error. Neural Architecture Search (NAS) automates this process by searching in a pre-defined search space (Elsken et al., 2019b). Previous work on NAS mainly focused on searching within a discrete search space by sampling a new architecture from the search space, evaluating its performance, and updating the optimizers (Zoph & Le, 2017; Zoph et al., 2018). However, training every network from scratch requires lots of GPU hours. One-Shot NAS (Pham et al., 2018) approaches instead share the same weights of the operators w.r.t. all the architectures in the search space. This allows to jointly optimize the architectures and weights. DARTS (Liu et al., 2019) and GDAS (Dong & Yang, 2019) further relax the discrete search space into continuous values to optimize the architecture parameters with gradient descent. The One-Shot NAS approach allows the optimizers to efficiently search for the optimal architecture within a huge search space. Similarly, NATS has multiple options for each token as the search space and is able to search for the optimal token types jointly with the model weights. However, unlike One-Shot NAS approaches that consider the optimization problem as a bilevel-optimization problem and optimize the model weights and architecture weights alternatively, we optimize the token state information and model weights within one forward and backward pass. This is similar to a mixture-of-expert (MOE) model (Shazeer et al., 2017; Fedus et al., 2023). However, instead of distributing data across all experts uniformly, we only select one expert for each token and assign all data to that expert.

3. The NATS Approach

In this section, we first introduce all the candidate token types in our search space. We then show that we can construct a learnable attention mask with the choice of each token type. Finally, we can efficiently reduce the KV cache size by dropping the unnecessary tokens during inference.

3.1. Search Space Design

Not all the tokens in a sequence are equally important. Some of the tokens might contain important information, and they should be preserved that will be further queried by the following tokens. Some tokens might only contribute to the

prediction for the next few tokens. Just like a paragraph is composed of multiple sentences, a sequence can be divided into multiple sub-sequences containing different information; some tokens might only be required within these sub-sequences. Hence, we design a search space for each token’s role within the sequence and ask the model to automatically learn the optimal role for each token in the sequence.

We first define **Global Token** as tokens containing important information that need to be preserved for the following predictions. Liu et al. (2023); Zhang et al. (2023b) showed that only a small fraction of the tokens contributes to most of the attention scores for self-attention computation. These tokens need to be preserved for models to recall the global information that helps to predict the next token. In vanilla transformer models, all the tokens are Global Tokens.

Global Tokens will not be evicted during inference time. Therefore, we should maintain as few Global Tokens as possible to ensure inference efficiency. Each Global Token should not only preserve the information within that position. Ideally, it should also be able to summarize the information from previous sequences (Guo et al., 2023; Chen et al., 2024). Hence, we split the entire sequence with the Global Tokens into multiple sub-sequences, with each sub-sequence ending with one Global Token. Each Global Token only needs to summarize the information from its sub-sequences and the previous Global Tokens.

Local Token only survives until the next Global Token appears. Therefore, models will have the full attention within each sub-sequence to summarize the local sub-sequence information into the Global Token located at the end of the sub-sequence while being sparse within the input sequence.

Only the Global Tokens and Local Tokens might control the sparsity at a low granularity level. E.g., assuming that one input sequence is highly localized, each token only has a high correlation with itself or a few neighboring tokens. In this case, they are all similar and are assigned with the same token type. However, none of the Global Token and Local Token could sparsify this attention map efficiently: if all the tokens are classified as Local Tokens, then the input sequence will only be considered as one single subsequence, and all the Local Tokens will be equivalent to the Global Tokens.

Hence, we introduce **Sliding Window Token**. Sliding Window Tokens will only be preserved for the next W time steps and were previously considered as one of the most popular sparse attention approaches (Child et al., 2019; Xiao et al., 2023; Zhang et al., 2023b; Ge et al., 2024).

In contrast to other causal attention maps, Figure 1(d) illustrates an exemplary attention mask constructed by the choices of different token types. In this case, we define the sliding window size as 4. Token 1, 4, 10 act as Global

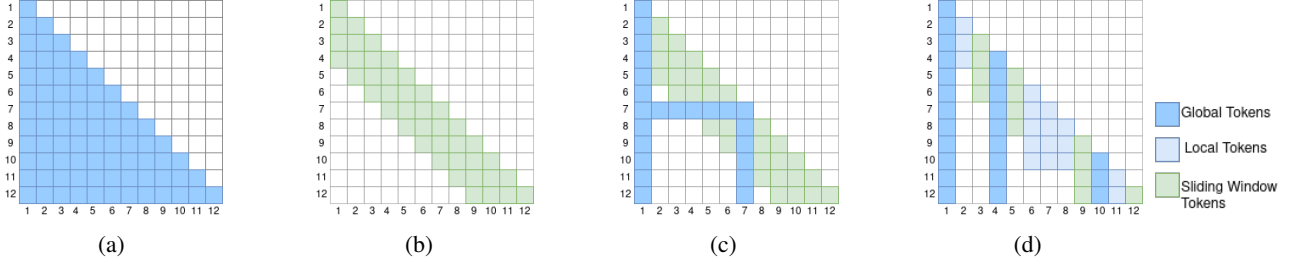


Figure 1. A comparison between different casual attention maps. 1(a): The full attention map, where each token is connected to the tokens before it. 1(b): the local attention with sliding windows 3, every token will only get access to the information of the 3 tokens ahead. 1(c) Longformer, besides the local attention, the first, 6th and 9th tokens are the pre-defined global tokens. 1(d): NATS dynamically searches for the optimal role for each token and constructs a learnable mask based on the roles for each token.

Tokens; Tokens 2, 6, 7, 8, 11 are Local Tokens; Token 3, 5, 9, 11 are Sliding Window Tokens. The Global Tokens splits the entire sequence into three subsequences that end at 4, 10, and the last index accordingly. Hence, Token 2 will only be queried by Token 3 and 4. This rule applies the same for Token 6, 7, and 8, where they only interact with the tokens within the same subsequence. For the sliding window tokens, only the next three tokens could query their information, regardless of whether these tokens belong to the same sub-sequence. Only 6 out of 12 tokens are involved during inference time to make the next token prediction.

3.2. Searching for the Optimal Token Types

Searching for the optimal token types within a sequence is similar to searching for the optimal architectures for a given task in neural architecture search (Elsken et al., 2019b; White et al., 2023). Following GDAS (Dong & Yang, 2019), we apply the Gumbel-Softmax trick (Jang et al., 2017; Madison et al., 2017) to sample from the discrete search space. The Gumbel-Softmax trick allows the gradient to be back-propagated through the discrete choice of the token types.

Specifically, we first use a linear layer (which we call Attention Score Layer) that maps each the input tensor for an attention layer $X \in \mathbb{R}^d$ to the likelihood for each option: $\alpha \in \mathbb{R}^{(H * N_{opts})} = \text{Linear}(\mathbf{x})$, where H is the number of KV heads and N_{opts} is the number of options in the search space. The type α for each token is then sampled from a Gumbel-Softmax function based on the likelihood values.

We could now construct a learnable attention mask M with a series of sampled token states. However, the additive mask in Eq. 1 will take $-\infty$ values, resulting in invalid gradient information. Hence, we use the token information to

construct a multiplicative attention mask $M^{mul} \in \{0, 1\}^1$:

$$O = \frac{e^A \odot M^{mul}}{\sum_j e^{A_{\cdot,j}} \odot M_{\cdot,j}^{mul}} V \quad (3)$$

The attention mask columns for Global Tokens and Sliding Window Tokens can be directly constructed since they will survive for a fixed amount of steps. However, the mask for Local Tokens $M_{i,j}^L$ is controlled by both the distribution from Local Tokens and Global Tokens as Local Tokens will survive until the next Global Token appears. In other words, to make $M_{i,j}^L (j > i)$ a valid value, no Global Token should appear between i and j .

Formally, the attention masks can be created as follows:

$$M_{i,j}^G = 1 \quad (4)$$

$$M_{i,j}^{SW} = \begin{cases} 1 & \text{if } j \leq i + W \\ 0 & \text{if } j > i + W \end{cases} \quad (5)$$

$$M_{i,j}^L = \prod_{n=j+1}^{i-1} (1 - G_n) \quad (6)$$

where W is the sliding window size and G_n a Global Token at Position n . We could then construct the attention masks based on the type of each token. After that, we mask out the upper triangular part of the mask to ensure its causality.

In practice, we first collect the index of the next global token $K_i := \min(\{k | k >= i \wedge G_k = 1\})$ and rewrite Eq. 6 as:

$$M_{i,j}^L = \begin{cases} 1 & \text{if } j \leq K_i \\ 0 & \text{if } j > K_i \end{cases} \quad (7)$$

These rules are then integrated in FlashAttention (Dao et al., 2022; Dao, 2024) to avoid explicitly computing the attention masks during the forward pass. In addition to the transformer computation, we only need to collect the next Global

¹For the sake of brevity, we will use M instead of M^{mul} in the following part of this paper.

Token indices \mathbf{K} (with a complexity of $\mathcal{O}(N)$) and then mask out the attention map values with the masks defined above.

To compute the gradients for M , we set $g(A, M) = e^A \odot M$; then the gradient for M is:

$$\frac{\partial O}{\partial M} = \frac{\partial O}{\partial g} \frac{\partial g}{\partial M} \quad \frac{\partial g}{\partial M} = e^A \quad \frac{\partial g}{\partial A} = e^A \odot M \quad (8)$$

Hence, the gradients for M are the same as those for A if M is 1. For the case of $M = 0$, this is the same as the values that $\partial O / \partial A$ is supposed to be if no learnable mask is applied to the attention map. Hence, we can jointly compute the gradient computation from both M and A within one backward pass. Further details can be found in the appendix.

The gradients towards each token are collected through the column sum of each value weighted by the corresponding attention masks:

$$d\alpha_i = \sum_j dM_{i,j} \times M_{i,j}^\alpha \quad (9)$$

Where $\alpha \in \{G, L, SW\}$ is the discretized token type. Intuitively, this shows the model's preference over short-range or long-range correlations: If i is quite close to j , then all the α will receive the same gradient information. However, if the model wants to create a long-range correlation with $i \gg j$, only Global Tokens will receive the gradient information and update their weights with the gradient.

Eq. 6 shows that the Global Token controls the local mask size. Therefore, the gradients for Global Token i should also be regularized by the gradient information from the previous tokens:

$$\frac{\partial M_{i,j}^L}{\partial G_k} = - \prod_{\substack{n=j+1 \\ n \neq k}}^{i-1} (1 - G_n) \quad (10)$$

In cases where G_k is 0, Equation 10 is the negative value of Equation 6. However, for the case where $G_k = 1$, this is equivalent to the local mask values where k is no longer set as a Global Token. This requires us to find the index of the next global token K_{k+1} and the last global token K_{k-l} where l is the length of the local sequence that ends at k .

This gradient information will then be collected and subtracted from the computed Global Tokens gradient values:

$$d\alpha_i^{G^-} = \begin{cases} \sum_{\substack{m \geq i \\ n < i}} M_{m,n}^L \times dM_{m,n} & \text{if } G_i = 0, \\ \sum_{\substack{K_{i+1} \geq m >= i \\ i > n \geq K_{k-l}}} dM_{m,n} & \text{if } G_i = 1, \end{cases} \quad (11)$$

$$d\alpha_i^G = d\alpha_i^G - d\alpha_i^{G^-} \quad (12)$$

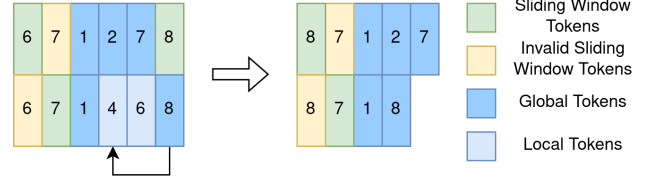


Figure 2. An example of how caches are updated within NATS when new tokens arrive with a model containing two heads. The two rows represent different heads.

Intuitively, this gradient term $d\alpha_i^{G^-}$ checks if the new Global Token needs to be inserted into the current sub-sequence (when G is 0) or we should remove the current Global Token to enlarge the current sub-sequence (when G is 1). We further illustrate this process in the appendix.

To control the attention map's sparsity, we introduce a small regularization value λ that is directly applied to the gradient for Global Token and Local Tokens to encourage more Sliding Window Tokens. We show how λ values control the attention map sparsity in the appendix.

3.3. Efficient Inference with Different Token Types

During inference time, we dynamically map the input feature maps to the corresponding token types and discard the tokens no longer required by the following tokens. The Sliding Window Tokens only survive for a fixed amount of time steps. We preserve a queue in the KV cache space that only stores the most recent W tokens and mask out the non-Sliding Window Tokens: when new tokens come, we place them after the tail of the queue to replace the tokens older than W .

Similar to the vanilla transformer forward process, when new tokens arrive, we concatenate them with the existing KV caches, generating new masks and computing the attention output. After that, we start our post-update process: we first check the state of each token to decide if we could remove them or keep them in the cached values. Since different heads might disagree on the types of the same token, we record both the sizes for Global Tokens ($Size_G$) and Local Tokens ($Size_L$) for all the heads. New Sliding Window Tokens do not change these sizes since they will always be placed separately. However, when a new Global Token for any head arrives, we remove all the Local Tokens from the corresponding heads and place the new Global Token right after the existing Global Tokens and then update our $Size_G$ and $Size_L$ accordingly. The same strategy is applied when new *LocalTokens* arrive: we place them at the end of the Local Tokens and increase the number for Local Tokens.

Figure 2 illustrates an exemplary case to update the KV caches in NATS with a sliding window size of 3. The first

two places store the most recent tokens and use a mask to mask out the non-Sliding Window Tokens (yellow tokens). Since the Token 8 for Head 1 is Sliding Window Token and Global Token for Head 2. We first move both tokens to the beginning of our cache to replace the old one. After that, we drop Token 8 in Head 1 since it has already moved to the sliding window caches. Then, since Token 8 in Head 2 is a Global Token, we drop all local tokens after the last Global Token (Token 1). Hence, Tokens 4 and 6 are removed from the cache, and we place Token 8 after Token 1. After that, the $Size_G$ is updated from $[5, 3]$ to $[5, 4]$ and the $Size_L$ is updated from $[0, 2]$ to $[0, 0]$. Since both new tokens are merged into the existing tokens, we do not need the extra space to store these new tokens.

4. Experiments

We implement NATS based on the Flash Attention 2 (Dao, 2024) implementation on triton. All the operations that we proposed in Section 3.2 have at most $O(L)$ complexity. In our experiments, we first train NATS parameters jointly within a transformer model from scratch. We then apply NATS to fine-tune a large language model.

4.1. Training a Transformer From Scratch

We first apply NATS to train a GPT2 small style (Radford et al., 2021) transformer model from scratch. Following the setting from NanoGPT (Karpathy, 2022), this model has 128M parameters with 12 layers and 12 heads with a hidden dimension of 768. Instead of the learnable position encoding, we apply rotary embeddings (Su et al., 2024) to each transformer layer. We train this model on the PG-19 Language Modeling Benchmark (Rae et al., 2020). This dataset contains books extracted from Project Gutenberg (PG19) with about 2B tokens in the training sets. We train all models with a context length of 1024 and batch size of 480 (using gradient accumulation). We train all models for 120 000 iterations on the training sets on a computation node with four Nvidia H100 GPUs. We evaluate all models on the test sets of PG19 with a context length of 1024.

As a baseline, we train another dense transformer model under the same hyperparameter setting. During inference time, we compare NATS with the following baselines besides the full Transformer: (i) Streaming LLM (Xiao et al., 2023) only preserves the first few starting and the most recent few tokens for future prediction. (ii) H2O (Zhang et al., 2023b) first computes the attention map and only preserves the tokens with the top-k attention scores. H2O and Streaming LLM are training-free approaches that control the sparsity with pre-defined hyperparameters during inference time. H2O needs to define the recent sliding window size and the number of Heavy Hitter (HH) tokens; Streaming LLM requires the number of tokens at the beginning of the se-

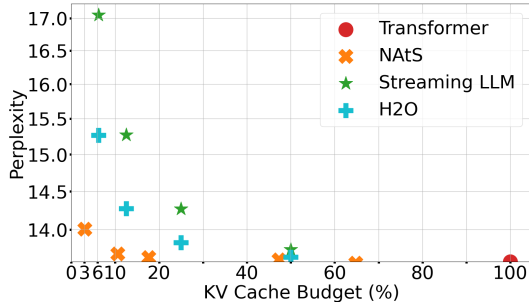


Figure 3. Perplexity vs KV Cache size under different sparsity settings λ on the PG19 dataset.

quence (Sink Tokens) and sliding window size. In contrast, NATS controls this sparsity by the sparsity hyperparameter value λ . Hence, we train multiple models with different λ . However, in our experiments, we observe that the attention map sparsity values converge much faster than the model loss. We could quickly estimate the attention map sparsity within the first 10,000 iterations to check if this sparsity value satisfies the user requirement and early-stop the runs that do not satisfy the requirements (Jamieson & Talwalkar, 2016).

We provide different hyperparameters for H2O and Streaming LLM (with the sliding window size of 32, 64, 128, and 256, plus the same number of HH/ Sink tokens). This results in a corresponding KV budget fraction ranging from 6.25% to 50%. Meanwhile, we train NATS with the following λ : $0, 1e-9, 5e-9, 1e-8, 1e-7$.

Figure 3 shows the perplexity of the PG19 test sets from different model settings. The x-axis indicates the fraction of KV caches applied to generate the last token in the input sequence. As expected, larger λ results in a smaller KV cache fraction. Interestingly, even if λ is set as 0, the KV cache budget can still be reduced to around 60% with slightly lower perplexity. This might indicate that the model also tends to sparsify the input information to focus more on the relevant parts from the input data (Ye et al., 2024).

Under the budget of around 50%, all the approaches perform similarly to the full transformer while NATS has a relatively lower perplexity and requires less budget. However, as the available budget decreases, NATS’s perplexity remains nearly the same until a KV cache size of around 10%. In contrast, H2O and Streaming LLM start to degenerate their performance starting from a 25% budget allocation. The most sparse model in NATS family only contains roughly 3% of the KV cache size (meaning roughly 30 cached tokens per layer on average) and achieves a lower perplexity compared to H2O with 12.5% of the KV caches and Streaming LLM with 25% of the KV caches.

4.2. Fine Tune a Large Language Models

We now apply NATs to fine-tune an existing large language model (Grattafiori et al., 2024; Jiang et al., 2023) in the long context scenario. We evaluate the fine-tuned models on the Needle-in-a-Haystack (NIAH) test (Kamradt, 2022) and LongBench dataset (Bai et al., 2024). NIAH places a random fact or statement (needle) in the middle of a long context and asks the model to retrieve it from the context. LongBench evaluates the model’s capacity to understand the information in different long context scenarios, such as single-document and multi-document QA, summarization, few-show learning, synthetic tasks, and code completion.

In addition to the baselines in Section 4.1, we use DuoAttention (Xiao et al., 2024) as another baseline. DuoAttention evaluates the importance of each attention head and only assigns full attention budgets to the heads with high scores (the so-called retrieval heads) while applying streaming to the other unimportant heads. DuoAttention shares the same idea as NATs, where the importance of different KV caches should be learned instead of the pre-defined rules. However, instead of learning the importance of the head level, we aim at learning this information directly on the token level.

To allow our models to learn to evaluate the role of each token within different contexts, we construct a new training dataset that follows the construction rules of LongBench. Some of LongBench’s tasks are collected from the test sets of the previous benchmarks. Hence, we first collect the training sets from these benchmarks and construct these datasets following the data structure in LongBench. Overall, this dataset contains 6 436 pieces of data with a maximum context length of 16 000. Further details on the dataset collection can be found in the appendix.

We only fine-tune the Attention Score Layer while keeping all the other parameters in the network fixed. Hence, we aim to approximate the original output from the corresponding base LLM. This approach is similar to DuoAttention (Xiao et al., 2024). However, since we want the model to capture the overall context information, we update Attention Score Layer with all the output from the full attention layer:

$$\mathcal{L}_{distill} = \frac{1}{B} \sum_{i=1}^B \sum_{j=1}^L (\mathbf{H}_{full}^{(i)}[j] - \mathbf{H}_{NAtS}^{(i)}[j])^2 \quad (13)$$

where B is the Batch Size. Additionally, we control the sparsity with the regularization value λ instead of the additional loss item defined in DuoAttention, and therefore, only optimize NATs with $\mathcal{L}_{distill}$ as the loss function. We fine-tune two long-context models (Llama-3-8B-Instruct-Gradient-1048k (Llama-3 8B Gradient Instruct 1048k) and Mistral-7B-v0.3-Instruct (Jiang et al., 2023)) on two Nvidia H100 GPUs for one epoch using AdamW (Kingma & Ba, 2015; Loshchilov & Hutter, 2019) with a learning rate of

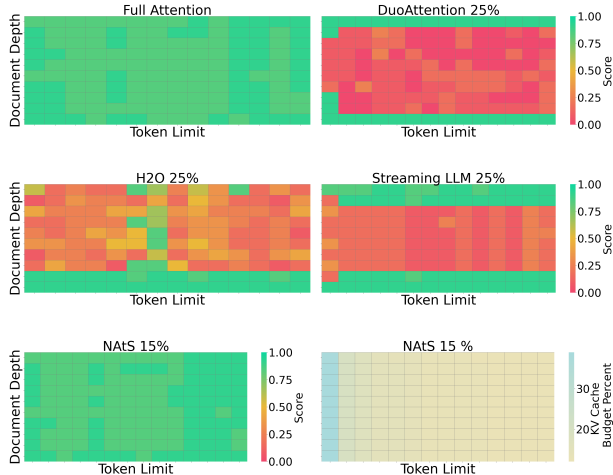


Figure 4. Results on Needle in a Haystack test with Llama-3-8B-Instruct-Gradient-1048k model. The context length ranges from 1 000 to 32 000 and the document depth ranges from 0 to 1. We assign a 25% budget to each of the approaches. The first two rows are the scores (higher is better) of the full attention and the corresponding baselines. The bottom plot on the left shows the scores from NATs with an average compression rate of 15%. The plot on the right shows the compression rate of NATs across different document lengths .

$3e-4$ with a warm-up from $3e-5$ in the first 20% steps and reducing back to $3e-5$ in the last 20% steps. We apply different λ to allow for different sparsity. For a fair comparison, we set the sliding window size W as 256, the same as DuoAttention.

Since we only optimize the Attention Score Layer, the number of learnable parameters is $n_{layers} \cdot d_{model} \cdot n_{heads} \cdot n_{options}$. Where $n_{options}$ is the number of options in our search space (in this case, it is 3). Hence, the size of the parameters that need to be stored is neglectable (it only takes roughly 13MB on disk for each set of Attention Score Layer) compared to the weights of the LLM. Hence, users could pre-collect all these weights and apply the one that fits their compression requirement.

For the Needle In a Haystack task, we test all models with a context length ranging from 1 000 to 32 000 with the needle positions ranging from 0 to 1. We assign a 25% KV cache budget to each of the baseline approaches. For NATs, we choose the model with the compression rate closest to 25%, which corresponds to a model trained with $\lambda = 1e - 7$ and an average KV budget size of 15%.

The results on Needle in a Haystack test are shown in Figure 4. DuoAttention, H2O, and Streaming LLM all maintain a sliding window with a fixed size. Therefore, they could well capture the needles inserted at the text’s tail. However, all the baselines struggle with the correct answers as

	Full	Duo	SLLM	H2O	NAtS
NarrativeQA	27.3	17.4	22.1	25.75	23.09(13%)
Qasper	28.9	16.4	13.0	16.9	29.01 (26%)
MultiFieldQA-en	52.3	35.8	40.6	29.1	48.72 (22%)
MultiFieldQA-zh	50.9	37.9	34.4	28.2	46.03 (27%)
HotpotQA	40.6	26.8	28.1	32.8	41.7 (17%)
2WikiQA	29.3	22.2	23.2	24.4	27.39 (20%)
Musique	24.4	12.0	17.9	18.1	21.0 (16%)
DuReader (zh)	30.2	26.3	31.3	17.7	28.44(20%)
GovReport	34.1	22.4	28.8	24.1	33.47 (20%)
QMSum	24.5	20.9	21.5	21.4	23.88 (15%)
MultiNews	27.7	24.0	24.4	22.4	27.77 (32%)
VCSUM (zh)	11.3	4.8	10.6	13.14	9.4(19%)
TREC	71.0	53.5	61.5	55.5	68.5 (22%)
TriviaQA	87.7	77.8	82.8	84.9	87.42 (18%)
SAMSum	42.5	41.0	39.4	38.8	41.78 (14%)
LSHT	38.0	21.5	25.0	22.2	35.5 (20%)
Passage Count	1.0	2.09	2.0	2.0	1.59(23%)
PassageRetrieval-en	80.5	46.5	25.5	47.0	67.0 (15%)
PassageRetrieval-zh	61.2	29.4	14.0	34.2	41.07 (24%)
LCC	37.5	36.2	43.5	44.74	40.11(35%)
RepoBench-P	38.0	39.1	42.0	41.9	42.63 (25%)

Table 1. LongBench Results with 25% Budget Allocation for full attention (Full), DuoAttention (Duo), Streaming LLM (SLLM), H2O and NATS on the LLama8B model. The numbers in the brackets for NATS is the used value KV cache sizes. We bold the models with the best performance besides the base Full Attention Models .

the needle goes into the middle of the context. In contrast, NATS efficiently recognizes the necessary tokens across different layers, heads and positions to preserve only tokens that contain the important information.

We also plot the KV budget percentage on the bottom right of Figure 4. Since we set our Sliding window size W as 256, the KV budget for the first 1000 tokens is roughly 30%. However, as the context length increases, the compression rates gradually decrease to the over compression rate of 15%. This shows NATS could save the important information uniformly across the context in different positions.

For the LongBench tasks, we evaluate all the baselines with the 50% and 25% of the KV cache sizes. We show the result with KV cache size of 25% for LLama3-8B in Table 1. The model that is used in this task is a model with $\lambda = 1e - 7$. NATS achieves the best performance on most of the dataset with (in many cases) smaller KV cache values. We provide further results, including results with Mistral-7B and NATS trained with other parameters, in the appendix.

4.2.1. KV SIZE DISTRIBUTION

Figure 5 shows the distribution of different KV budgets on the narrativeQA (Kociský et al., 2018) and RepoBench-P (Liu et al., 2024) dataset. The overall trends are similar: The first few layers and some specific heads require more layers than the other heads. However, as the model goes

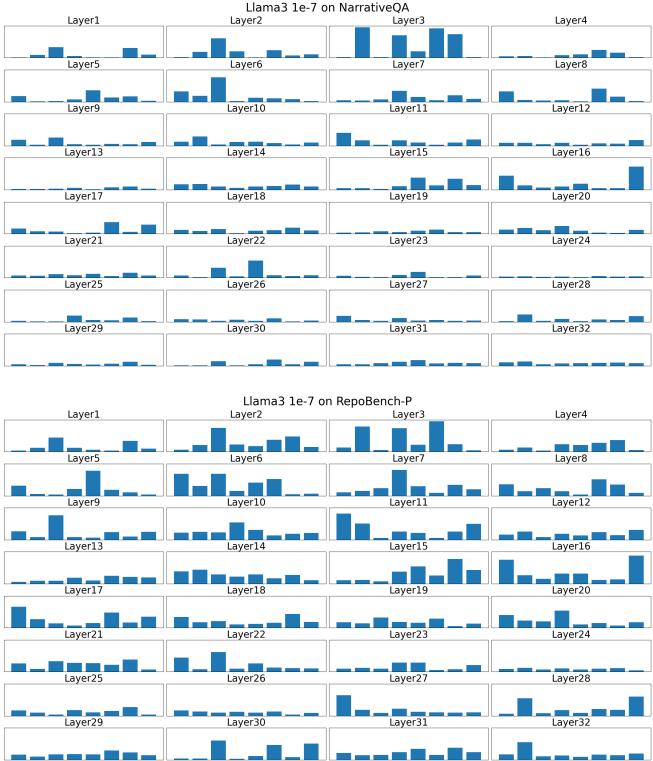


Figure 5. KV cache size compression on different layers

deeper, the model tends to drop more tokens for the NarrativeQA dataset while still maintaining many tokens for RepoBench-P, especially after layer 16. This shows that a fixed rule might not always fit all the sequences and there is a need to adjust the sampling strategy with different inputs.

5. Conclusion and Future Work

Efficiently managing the KV cache is crucial for deploying large language models in long-context applications. In this work, we propose NATS, an approach that automatically optimizes the optimal roles of each token to determine how long they should survive. By constructing a learnable mask, NATS learns to sparsify the attention map end-to-end. Our experiments show that NATS could use much less KV caches compared to the State-of-the-art KV caching reduction approach. While NATS shows promising results, future work could include exploration of further token roles and structured search spaces with hierarchies. Overall, we believe that NATS paves the way towards more efficient and scalable inference with LLMs.

6. Impact Statements

LLMs are widely applied to different fields nowadays. However, the cost for LLM to store the KV cache and predict

the next token is still huge, given the $O(L)$ computation and memory costs of full Attention Models. This prevents further adaptation of LLMs (and other transformer-based foundation models with properties similar to those described before) because of high energy consumption and limited context windows. NATS achieves a substantial reduction in KV cache size with minimal impact on model performance, outperforming existing state-of-the-art approaches. This increased efficiency can enable the deployment of larger, more powerful language models on resource-constrained devices and facilitate the development of new applications that rely on long-context understanding, such as advanced conversational AI, comprehensive document summarization, and complex code generation. By making long-context processing more accessible, NATS has the potential to accelerate progress in natural language processing and related fields. Nevertheless, it does not solve other inherent problems of LLMs such as hallucinations.

7. Acknowledgement

The authors gratefully acknowledge the computing time provided to them on the high-performance computers Noc-tua2 at the NHR Center PC2 under the project hpc-prf-intexml. These are funded by the Federal Ministry of Education and Research and the state governments participating on the basis of the resolutions of the GWK for the national high performance computing at universities (www.nhr-verein.de/unsere-partner).

Difan Deng was supported by the Federal Ministry of Education and Research (BMBF) under the project AI service center KISSKI (grantno.01IS22093C).

References

- Proceedings of the International Conference on Learning Representations (ICLR'17)*, 2017. Published online: iclr.cc.
- Proceedings of the International Conference on Learning Representations (ICLR'19)*, 2019. Published online: iclr.cc.
- Proceedings of the 37th International Conference on Advances in Neural Information Processing Systems (NeurIPS'23)*, 2023. Curran Associates.
- International Conference on Learning Representations (ICLR'24)*, 2024. Published online: iclr.cc.
- Forty-first International Conference on Machine Learning*, 2024.
- Anagnostidis, S., Pavllo, D., Biggio, L., Noci, L., Lucchi, A., and Hofmann, T. Dynamic context pruning for efficient and interpretable autoregressive transformers. In *Proceedings of the 37th International Conference on Advances in Neural Information Processing Systems (NeurIPS'23)* [neu \(2023\)](https://openreview.net/forum?id=uvdJgFFzby). URL <https://openreview.net/forum?id=uvdJgFFzby>.
- Anthropic. The claude 3 model family: Opus, sonnet, haiku, 2024. URL https://www-cdn.anthropic.com/de8ba9b01c9ab7cbabf5c33b80b7bbc618857627/Model_Card_Claude_3.pdf.
- Bai, Y., Lv, X., Zhang, J., Lyu, H., Tang, J., Huang, Z., Du, Z., Liu, X., Zeng, A., Hou, L., Dong, Y., Tang, J., and Li, J. LongBench: A bilingual, multitask benchmark for long context understanding. In Ku, L., Martins, A., and Srikumar, V. (eds.), *Proceedings of the 62nd Annual Meeting of the Association for Computational Linguistics*, pp. 3119–3137. Association for Computational Linguistics, 2024.
- Beltagy, I., Peters, M. E., and Cohan, A. Longformer: The long-document transformer. *arXiv:2004.05150 [cs.CL]*, 2024.
- Brown, T., Mann, B., Ryder, N., Subbiah, M., Kaplan, J., Dhariwal, P., Neelakantan, A., Shyam, P., Sastry, G., Askell, A., Agarwal, S., Herbert-Voss, A., Krueger, G., Henighan, T., Child, R., Ramesh, A., Ziegler, D., Wu, J., Winter, C., Hesse, C., Chen, M., Sigler, E., Litwin, M., Gray, S., Chess, B., Clark, J., Berner, C., McCandlish, S., Radford, A., Sutskever, I., and Amodei, D. Language models are few-shot learners. In Larochelle, H., Ranzato, M., Hadsell, R., Balcan, M.-F., and Lin, H. (eds.), *Proceedings of the 34th International Conference on Advances in Neural Information Processing Systems (NeurIPS'20)*, pp. 1877–1901. Curran Associates, 2020.
- Cai, Z., Zhang, Y., Gao, B., Liu, Y., Liu, T., Lu, K., Xiong, W., Dong, Y., Chang, B., Hu, J., and Xiao, W. Pyramidkv: Dynamic KV cache compression based on pyramidal information funneling. *arXiv: 2406.02069 [cs.CL]*, 2024.
- Chen, G., Shi, H., Li, J., Gao, Y., Ren, X., Chen, Y., Jiang, X., Li, Z., Liu, W., and Huang, C. Sepllm: Accelerate large language models by compressing one segment into one separator, 2024. URL <https://arxiv.org/abs/2412.12094>.
- Child, R., Gray, S., Radford, A., and Sutskever, I. Generating long sequences with sparse transformers. *arXiv:1904.10509 [cs.LG]*, 2019.
- Dao, T. FlashAttention-2: Faster attention with better parallelism and work partitioning. In *International Conference on Learning Representations (ICLR'24)* [iclr \(2024\)](https://iclr.cc). Published online: iclr.cc.

- Dao, T., Fu, D., Ermon, S., Rudra, A., and Ré, C. FlashAttention: Fast and memory-efficient exact attention with io-awareness. *Advances in Neural Information Processing Systems*, 35:16344–16359, 2022.
- Dasigi, P., Lo, K., Beltagy, I., Cohan, A., Smith, N., and Gardner, M. A dataset of information-seeking questions and answers anchored in research papers. In [Toutanova et al. \(2021\)](#), pp. 4599–4610.
- Dong, X. and Yang, Y. Searching for a robust neural architecture in four gpu hours. In *Proceedings of the International Conference on Computer Vision and Pattern Recognition (CVPR’19)*. Computer Vision Foundation and IEEE Computer Society, IEEE, 2019.
- Elsken, T., Metzen, J., and Hutter, F. Neural Architecture Search. In Hutter, F., Kotthoff, L., and Vanschoren, J. (eds.), *Automated Machine Learning: Methods, Systems, Challenges*, chapter 3, pp. 63–77. Springer, 2019a. Available for free at <http://automl.org/book>.
- Elsken, T., Metzen, J., and Hutter, F. Neural Architecture Search: A survey. *Journal of Machine Learning Research*, 20(55):1–21, 2019b.
- Fabbri, A., Li, I., She, T., Li, S., and Radev, D. Multi-news: A large-scale multi-document summarization dataset and abstractive hierarchical model. In Burstein, J., Doran, C., and Solorio, T. (eds.), *Proceedings of the 2019 Conference of the North American Chapter of the Association for Computational Linguistics: Human Language Technologies*, pp. 1074–1084. Association for Computational Linguistics, 2019.
- Fedus, W., Zoph, B., and Shazeer, N. Switch transformers: Scaling to trillion parameter models with simple and efficient sparsity. *Journal of Machine Learning Research (JMLR)*, 2023.
- Feng, Y., Lv, J., Cao, Y., Xie, X., and Zhou, S. Ada-kv: Optimizing KV cache eviction by adaptive budget allocation for efficient LLM inference. *arXiv: 2407.11550 [cs.CL]*, abs/2407.11550, 2024.
- Ge, S., Zhang, Y., Liu, L., Zhang, M., Han, J., and Gao, J. Model tells you what to discard: Adaptive KV cache compression for llms. In *International Conference on Learning Representations (ICLR’24) icl (2024)*. Published online: iclr.cc.
- Gemini, T. and et al. Gemini: A family of highly capable multimodal models. *arXiv:2312.11805 [cs.CL]*, 2024.
- Gliwa, B., Mochol, I., Biesek, M., and Wawer, A. Samsun corpus: A human-annotated dialogue dataset for abstractive summarization. *arXiv: 1911.12237 [cs.CL]*, 2019.
- Grattafiori, A., Dubey, A., Jauhri, A., Pandey, A., Kadian, A., Al-Dahle, A., Letman, A., and et al. The llama 3 herd of models, 2024. URL <https://arxiv.org/abs/2407.21783>.
- Guo, D., Xu, C., Duan, N., Yin, J., and McAuley, J. Long-coder: A long-range pre-trained language model for code completion. In Krause, A., Brunskill, E., Cho, K., Engelhardt, B., Sabato, S., and Scarlett, J. (eds.), *Proceedings of the 40th International Conference on Machine Learning (ICML’23)*, volume 202 of *Proceedings of Machine Learning Research*, pp. 12098–12107. PMLR, 2023. URL <https://proceedings.mlr.press/v202/guo23j.html>.
- He, W., Liu, K., Liu, J., Lyu, Y., Zhao, S., Xiao, X., Liu, Y., Wang, Y., Wu, H., She, Q., Liu, X., Wu, T., and Wang, H. Dureader: a chinese machine reading comprehension dataset from real-world applications. In *Proceedings of the Workshop on Machine Reading for Question Answering@ACL 2018, Melbourne, Australia, July 19, 2018*, pp. 37–46, 2018. URL <https://aclanthology.org/w18-2605/>.
- Ho, X., Nguyen, A. D., Sugawara, S., and Aizawa, A. Constructing A multi-hop QA dataset for comprehensive evaluation of reasoning steps. In Scott, D., Bel, N., and Zong, C. (eds.), *Proceedings of the 28th International Conference on Computational Linguistics, COLING 2020*, pp. 6609–6625. International Committee on Computational Linguistics, 2020.
- Huang, L., Cao, S., Parulian, N. N., Ji, H., and Wang, L. Efficient attentions for long document summarization. In [Toutanova et al. \(2021\)](#), pp. 1419–1436.
- Jamieson, K. and Talwalkar, A. Non-stochastic best arm identification and Hyperparameter Optimization. In Gretton, A. and Robert, C. (eds.), *Proceedings of the Seventeenth International Conference on Artificial Intelligence and Statistics (AISTATS’16)*, volume 51. Proceedings of Machine Learning Research, 2016.
- Jang, E., Gu, S., and Poole, B. Categorical reparameterization with gumbel-softmax. In *Proceedings of the International Conference on Learning Representations (ICLR’17) icl (2017)*. Published online: iclr.cc.
- Jiang, A., Sablayrolles, A., Mensch, A., Bamford, C., Chaplot, D., de las Casas, D., and et al. Mistral 7b, 2023.
- Joshi, M., Choi, E., Weld, D., and Zettlemoyer, L. Triviaqa: A large scale distantly supervised challenge dataset for reading comprehension. In Barzilay, R. and Kan, M.-Y. (eds.), *Proceedings of the 55th Annual Meeting of the Association for Computational Linguistics (Volume 2: Short Papers)*, pp. 1601–1611. Association for Computational Linguistics, 2017.

- Kamradt, G. NanoGPT. https://github.com/gkamradt/LLMTest_NeedleInAHaystack, 2022.
- Karpathy, A. NanoGPT. <https://github.com/karpathy/nanoGPT>, 2022.
- Kim, S., Shen, S., Thorsley, D., Gholami, A., Kwon, W., Hassoun, J., and Keutzer, K. Learned token pruning for transformers. In Zhang, A. and Rangwala, H. (eds.), *Proceedings of the 28th ACM SIGKDD International Conference on Knowledge Discovery and Data Mining (KDD'22)*, pp. 784–794. ACM Press, 2022. URL <https://doi.org/10.1145/3534678.3539260>.
- Kingma, D. and Ba, J. Adam: A method for stochastic optimization. In *Proceedings of the International Conference on Learning Representations (ICLR'15)*, 2015. Published online: iclr.cc.
- Kociský, T., Schwarz, J., Blunsom, P., Dyer, C., Hermann, K., Melis, G., and Grefenstette, E. The narrativeqa reading comprehension challenge. *Transactions of the Association for Computational Linguistics*, 6:317–328, 2018. URL https://doi.org/10.1162/tacl_a_00023.
- Li, X. and Roth, D. Learning question classifiers. In *19th International Conference on Computational Linguistics, COLING*, 2002.
- Li, Y., Huang, Y., Yang, B., Venkitesh, B., Locatelli, A., Ye, H., Cai, T., Lewis, P., and Chen, D. Snapkv: LLM knows what you are looking for before generation. *arXiv:2404.14469 [cs.CL]*, 2024.
- Liu, H., Simonyan, K., and Yang, Y. DARTS: Differentiable architecture search. In *Proceedings of the International Conference on Learning Representations (ICLR'19) icl (2019)*. Published online: iclr.cc.
- Liu, T., Xu, C., and McAuley, J. Repobench: Benchmarking repository-level code auto-completion systems, 2024. URL <https://arxiv.org/abs/2306.03091>. Published online: iclr.cc.
- Liu, Z., Desai, A., Liao, F., Wang, W., Xie, V., Xu, Z., Kyrillidis, A., and Shrivastava, A. Scissorhands: Exploiting the persistence of importance hypothesis for LLM KV cache compression at test time. In *Proceedings of the 37th International Conference on Advances in Neural Information Processing Systems (NeurIPS'23) neu (2023)*. URL <https://openreview.net/forum?id=JZfg6wGi6g>.
- Llama-3 8B Gradient Instruct 1048k. <https://huggingface.co/gradientai/Llama-3-8B-Instruct-Gradient-1048k>.
- Loshchilov, I. and Hutter, F. Decoupled weight decay regularization. In *Proceedings of the International Conference on Learning Representations (ICLR'19) icl (2019)*. Published online: iclr.cc.
- Lou, C., Jia, Z., Zheng, Z., and Tu, K. Sparser is faster and less is more: Efficient sparse attention for long-range transformers. *arXiv:2406.16747, [cs.CL]*, abs/2406.16747, 2024. URL <https://doi.org/10.48550/arXiv.2406.16747>.
- Maddison, C., Mnih, A., and Y.Teh. The concrete distribution: A continuous relaxation of discrete random variables. In *Proceedings of the International Conference on Learning Representations (ICLR'17) icl (2017)*. URL <https://openreview.net/forum?id=S1jE5L5gl>. Published online: iclr.cc.
- Mohtashami, A. and Jaggi, M. Random-access infinite context length for transformers. In *Proceedings of the 37th International Conference on Advances in Neural Information Processing Systems (NeurIPS'23) neu (2023)*. URL <https://openreview.net/forum?id=7eHn64wOVy>.
- Nawrot, P., Chorowski, J., Lancucki, A., and Ponti, E. Efficient transformers with dynamic token pooling. In Rogers, A., Boyd-Graber, J., and Okazaki, N. (eds.), *Proceedings of the 61st Annual Meeting of the Association for Computational Linguistics*, pp. 6403–6417. Association for Computational Linguistics, 2023. URL <https://doi.org/10.18653/v1/2023.acl-long.353>.
- Nawrot, P., Lancucki, A., Chochowski, M., Tarjan, D., and Ponti, E. Dynamic memory compression: Retrofitting llms for accelerated inference. In *Forty-first International Conference on Machine Learning icm (2024)*.
- PG19. <https://www.gutenberg.org/>.
- Pham, H., Guan, M., Zoph, B., Le, Q., and Dean, J. Efficient Neural Architecture Search via parameter sharing. In Dy, J. and Krause, A. (eds.), *Proceedings of the 35th International Conference on Machine Learning (ICML'18)*, volume 80. Proceedings of Machine Learning Research, 2018.
- Radford, A., Kim, J. W., Hallacy, C., Ramesh, A., Goh, G., Agarwal, S., Sastry, G., Askell, A., Mishkin, P., Clark, J., et al. Learning transferable visual models from natural language supervision. *arXiv:2103.00020v1 [cs.CV]*, 2021.
- Rae, J., Potapenko, A., Jayakumar, S., Hillier, C., and Lillicrap, T. Compressive transformers for long-range sequence modelling. In *Proceedings of the International*

- Conference on Learning Representations (ICLR'20)*, 2020. URL <https://openreview.net/forum?id=SylKikSYDH>. Published online: [iclr.cc](https://arxiv.org/abs/2005.00147).
- Shazeer, N., Mirhoseini, A., Maziarz, K., Davis, A., Le, Q., Hinton, G., and Dean, J. Outrageously large neural networks: The sparsely-gated mixture-of-experts layer. In *Proceedings of the International Conference on Learning Representations (ICLR'17) icl (2017)*. Published online: [iclr.cc](https://arxiv.org/abs/1701.07867).
- Su, J., Ahmed, M., Lu, Y., Pan, S., Bo, W., and Liu, Y. Roformer: Enhanced transformer with rotary position embedding. *Neurocomputing*, pp. 127063, 2024. URL <https://doi.org/10.1016/j.neucom.2023.127063>.
- Toutanova, K., Rumshisky, A., Zettlemoyer, L., Hakkani-Tür, D., Beltagy, I., Bethard, S., Cotterell, R., Chakraborty, T., and Zhou, Y. (eds.). *Proceedings of the 2021 Conference of the North American Chapter of the Association for Computational Linguistics: Human Language Technologies, NAACL-HLT 2021, Online, June 6-11, 2021*, 2021. Association for Computational Linguistics.
- Trivedi, H., Balasubramanian, N., Khot, T., and Sabharwal, A. Musique: Multihop questions via single-hop question composition. *Trans. Assoc. Comput. Linguistics*, 10:539–554, 2022.
- Vaswani, A., Shazeer, N., Parmar, N., Uszkoreit, J., Jones, L., Gomez, A., Kaiser, L., and Polosukhin, I. Attention is all you need. In Guyon, I., von Luxburg, U., Bengio, S., Wallach, H., Fergus, R., Vishwanathan, S., and Garnett, R. (eds.), *Proceedings of the 31st International Conference on Advances in Neural Information Processing Systems (NeurIPS'17)*. Curran Associates, Inc., 2017.
- White, C., Safari, M., Sukthanker, R., Ru, B., Elsen, T., Zela, A., Dey, D., and Hutter, F. Neural architecture search: Insights from 1000 papers. *arXiv:2301.08727 [cs.LG]*, 2023.
- Wu, H., Zhan, M., Tan, H., Hou, Z., Liang, D., and Song, L. VCSUM: A versatile chinese meeting summarization dataset. In Rogers, A., Boyd-Graber, J. L., and Okazaki, N. (eds.), *Findings of the Association for Computational Linguistics: ACL 2023*, pp. 6065–6079. Association for Computational Linguistics, 2023.
- Xiao, G., Tian, Y., Chen, B., Han, S., and Lewis, M. Efficient streaming language models with attention sinks. *arXiv:2309.17453 [cs.CL]*, 2023.
- Xiao, G., Tang, J., Zuo, J., Guo, J., Yang, S., Tang, H., Fu, Y., and Han, S. Duoattention: Efficient long-context llm inference with retrieval and streaming heads. *arXiv:2410.10819 [cs.CL]*, 2024.
- Yang, Z., Qi, P., Zhang, S., Bengio, Y., Cohen, W., Salakhutdinov, R., and Manning, C. D. Hotpotqa: A dataset for diverse, explainable multi-hop question answering. In Riloff, E., Chiang, D., Hockenmaier, J., and Tsujii, J. (eds.), *Proceedings of the 2018 Conference on Empirical Methods in Natural Language Processing*, pp. 2369–2380. Association for Computational Linguistics, 2018.
- Ye, T., Dong, L., Xia, Y., Sun, Y., Zhu, Y., Huang, G., and Wei, F. Differential transformer, 2024.
- Yi, Z., Ouyang, J., Liu, Y., Liao, T., Xu, Z., and Shen, Y. A survey on recent advances in llm-based multi-turn dialogue systems. *arXiv: 2402.18013 [cs.CL]*, abs/2402.18013, 2024.
- Zhang, T., Ladhak, F., Durmus, E., Liang, P., McKeown, K., and Hashimoto, T. Benchmarking large language models for news summarization, 2023a. URL <https://arxiv.org/abs/2301.13848>.
- Zhang, Y., Du, Y., Luo, G., Zhong, Y., Zhang, Z., Liu, S., and Ji, R. Cam: Cache merging for memory-efficient llms inference. In *Forty-first International Conference on Machine Learning icm (2024)*. URL <https://openreview.net/forum?id=LCTmppB165>.
- Zhang, Z., Sheng, Y., Zhou, T., Chen, T., Zheng, L., Cai, R., Song, Z., Tian, Y., Ré, C., Barrett, C. W., Wang, Z., and Chen, B. H2O: heavy-hitter oracle for efficient generative inference of large language models. In *Proceedings of the 37th International Conference on Advances in Neural Information Processing Systems (NeurIPS'23) neu (2023)*. URL <https://openreview.net/forum?id=RkRrPp7GKO>.
- Zhong, M., Yin, D., Yu, T., Zaidi, A., Mutuma, M., Jha, R., Awadallah, A., Celikyilmaz, A., Liu, Y., Qiu, X., and Radev, D. Qmsum: A new benchmark for query-based multi-domain meeting summarization. In *Toutanova et al. (2021)*, pp. 5905–5921.
- Zoph, B. and Le, Q. V. Neural Architecture Search with reinforcement learning. In *Proceedings of the International Conference on Learning Representations (ICLR'17) icl (2017)*. Published online: [iclr.cc](https://arxiv.org/abs/1703.01571).
- Zoph, B., Vasudevan, V., Shlens, J., and Le, Q. Learning transferable architectures for scalable image recognition. In *Proceedings of the International Conference on Computer Vision and Pattern Recognition (CVPR'18)*. Computer Vision Foundation and IEEE Computer Society, IEEE, 2018.

A. Details on Backward Propagation

A.1. Gradients for Attention Masks

$$\frac{\partial O}{\partial M} = \frac{\partial O}{\partial g} \frac{\partial g}{\partial M} \quad (14)$$

$$\frac{\partial g}{\partial M} = e^A \quad (15)$$

$$\frac{\partial g}{\partial A} = e^A \odot M \quad (16)$$

In Eq. 15 and 16, we show the gradient for M is the same as the value that $\partial O/\partial A$ is supposed to be if no mask is applied. Since we have $g_{i,j} = e^{A_{i,j}} \odot M_{i,j}$. Let's set $S_i := \sum_j g_{i,j}$ and $P_{i,j} := \frac{g_{i,j}}{S_i}$. Then we have $d\mathbf{P} = d\mathbf{O}\mathbf{V}^T$. Therefore,

$$dg_{i:} = (\text{diag}(\frac{1}{S_{i:}}) - \frac{1}{S_{i:}} P_{i:}^T) dP_{i:} \quad (17)$$

Combining Eq. 17 with Eq. 16 and Eq. 15 provides the same gradients as the vanilla softmax function with additive masks:

$$dM_{i:} = (\text{diag}(\frac{e^{A_{i:}}}{S_{i:}}) - \frac{e^{A_{i:}}}{S_{i:}} P_{i:}^T) dP_{i:} \quad (18)$$

$$\begin{aligned} dA &= dM \odot M \\ &= (\text{diag}(P_{i:}) - P_{i:} P_{i:}^T) dP_{i:} \end{aligned} \quad (19)$$

Since $dg_{i:}$ is required to compute the gradient for $\mathbf{A}_{i:}$ and always needs to be computed. We can directly use this information to compute the gradients for the attention Mask M .

Following FlashAttention (Dao et al., 2022), we define $D_i = do_i^T o_i$, then

$$dM = \frac{e^{A_{i,j}}}{S_{i:}} (dP_{ij} - D_i) \quad (20)$$

$$dA_{i,j} = P_{i,j} (dP_{ij} - D_i) \quad (21)$$

and dA is computed by Eq. 19. After that, we can backpropagate dA to dq and dv . Since M needs to be recomputed anyway in the flash attention's backward process, this only results in little computational overhead.

However, in practice, we found this makes the training unstable. All the values in a row with vanilla softmax attention are normalized such that their sum is bounded. However, we need to use the unmasked e^M to compute dM in our scenerio, meaning $\frac{e^{A_{i,j}}}{S_i}$ could be unbounded. This might result in an unstable training process. To alleviate this, we record both the masked denominator S_i and unmasked denominator $S'_i = \sum_j e^{A_{i,j}}$ during the forward pass. We then use the unmasked denominator to compute the unmasked $P'_{i,j} = \frac{e^{A_{i,j}}}{S'_i}$ and further apply p' to compute dM :

$$dM = P'_{i,j} (dP_{ij} - D_i) \quad (22)$$

This only requires storing an additional S'_i during the forward pass (with a complexity of $O(L)$) and one additional computation during the backward pass (since S'_i is already computed and stored during the forward pass).

A.2. Details on computing $d\alpha_i^{G-}$

In Eq. 11 and 12, we show that an additional $d\alpha_i^{G-}$ needs to be computed for each token's gradient for Global Tokens. Figure 6 illustrates an example of this. Token 4 is a global token, and we search for its next Global Token (which is Token 10 in this example). Assuming that we want to change Token 4 to another role, the regions within the boundary (orange ones) are those tokens that are influenced by this switching: given that Token 4 no longer becomes Global Token, Token 2 and 3

will be part of a larger subsequence that ranges from 1 to 10, and the attentino maps within the orange region should not be masked out. Intuitively, this gradient measures the regret that we made in order to switch one Global Token into a Local Token. A similar idea can be found in the red region. Assuming that we want to switch Token 7 to a Global Token, then Tokens 5,6 will be split into a new subsequence and we will no longer connect them with Token 8, 9, 10 since they belong to two different sub-sequences after the switch. Hence, this value in the red regions measures the regret if we mistakenly classify a Global Token as non-Global Tokens.

In practice, the $d\alpha_i^{G-}$ values for Global Token can be easily collected since we can easily get the last and next G index with a scan function and collect the gradients to the corresponding positions. However, for those values on non Global Tokens, since the entire sequence can be a sub-sequence if no Global Token exists in the current sequence, collecting all the values that are below and on the left side of the Local Tokens might be too expensive. Hence, we ask each Local Token can only visit a fixed number of tokens on both sides. In this case, this operation is equivalent to a convolutional operation with weights of either 1 or 0. We set this value as 16 in our experiments to fit the grid sizes in triton.

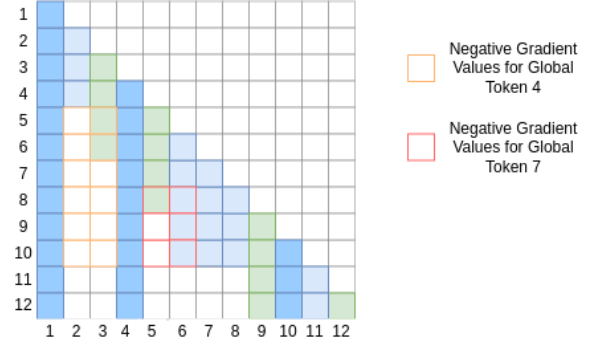


Figure 6. The gradient term $d\alpha_i^{G-}$ for Token 4 and 7

A.3. Optimizing for sparser Attention Maps

The sparse regularization term λ is directly applied to the corresponding gradients for the Global Tokens and Local Tokens. This value should penalize the number of unmasked tokens for each row. While the number of unmasked tokens for Global Token and Local Tokens in column i are $L - i$ and $K_i - i$ with K_i defined in Section 3.2. Hence, we have:

$$dG_i^{G_{sparse}} = \lambda \times \frac{L - i}{L} \quad (23)$$

$$dG_i^{L_{sparse}} = \lambda \times \frac{K_i - i}{L} \quad (24)$$

Combining Eq. 9, 11, 23 and Eq. 24, we have:

$$d\alpha_i^G = \sum_j dM_{i,j} \times M_{i,j}^G \times M_{i,j}^{casual} + dG_i^{G_{sparse}} - d\alpha_i^{G-} \quad (25)$$

$$d\alpha_i^L = \sum_j dM_{i,j} \times M_{i,j}^L \times M_{i,j}^{casual} + dG_i^{L_{sparse}} \quad (26)$$

$$d\alpha_i^{SW} = \sum_j dM_{i,j} \times M_{i,j}^{SW} \times M_{i,j}^{casual} \quad (27)$$

with $M_{i,j}^G, M_{i,j}^{SW}, M_{i,j}^L$ defined in Eq. 4, 7 and 5 and $M_{i,j}^{casual}$ is a casual attention mask.

B. Experiments Details

B.1. Collecting the Fine-tune Training Set

To fine-tune NAtS on LLMs, we collect the training datasets from different tasks:

- Multi-Document QA: HotPotQA (Yang et al., 2018), 2WikiMultihopQA (Ho et al., 2020), MuSiQue (Trivedi et al., 2022), and DuReader (zh) (He et al., 2018)
- Single-Document QA: NarrativeQA (Kociský et al., 2018) and Qasper (Dasigi et al., 2021)
- Summarization: GovReport (Huang et al., 2021), QMSum (Zhong et al., 2021), MultiNews (Fabbri et al., 2019), and VCSUM (zh) (Wu et al., 2023)
- Few-shot Learning: TREC (Li & Roth, 2002), TriviaQA (Joshi et al., 2017), and SAMSum (Gliwa et al., 2019)
- Code Completion: LCC (Guo et al., 2023) and RepoBench-P (Liu et al., 2024)

For all the few-shot learning datasets, following Bai et al. (2024), we randomly concatenate multiple question-answer pairs into one single extended context as one piece of data. The number of concatenated samples for the TREC dataset ranges from [10, 100]. This value is [2, 6] for TriviaQA and [10, 50] for SAMSum. Additionally, for the dataset that do not have enough context length (e.g., the DuReader dataset), we also merge multiple documents into one piece of data (in our case, this value is 4).

We do not collect all the data whose length goes beyond a threshold to ensure that the context can be fitted into our model. Additionally, we collect at most 500 pieces of data in each dataset since some datasets might not contain pieces of data. In the end, this training set contains 6436 pieces of data in total.

	Full	Duo	SLLM	H2O	NAtS
NarrativeQA	29.2	16.5	21.9	23.6	26.84 (14%)
Qasper	41.3	14.6	18.0	18.9	41.05 (27%)
MultiFieldQA-en	52.5	29.8	39.9	31.5	53.07 (24%)
MultiFieldQA-zh	58.0	29.1	41.6	29.2	55.47 (19%)
HotpotQA	49.6	34.9	34.2	42.1	53.02 (22%)
2WikiQA	40.0	27.8	31.1	30.4	37.22 (25%)
Musique	28.4	13.0	16.4	17.0	26.29 (21%)
DuReader (zh)	34.9	26.5	34.4	20.7	34.4 (15%)
GovReport	34.9	22.1	30.3	27.1	33.31 (20%)
QMSum	25.7	17.2	21.2	20.8	25.48 (19%)
MultiNews	27.9	23.4	23.6	23.0	27.32 (35%)
VCSUM (zh)	16.3	13.6	14.6	15.1	16.21 (13%)
TREC	75.5	52.0	69.0	61.5	73.0 (29%)
TriviaQA	88.9	84.8	85.0	86.6	88.8 (23%)
SAMSum	47.3	42.1	45.0	45.2	45.68 (19%)
LSHT	39.8	17.5	26.0	22.0	39.75 (15%)
Passage Count	5.5	3.5	3.5	6.0	4.56(22%)
PassageRetrieval-en	98.0	62.5	30.5	63.0	57.5(19%)
PassageRetrieval-zh	96.5	10.5	22.0	34.5	58.07 (17%)
LCC	50.7	48.8	46.4	50.5	51.27 (36%)
RepoBench-P	54.8	46.4	49.8	53.8	55.98 (30%)

Table 2. LongBench Results with 25% Budget Size on Mistral-7B. .

C. Further Results on LongBench Dataset

We show additional results on fine-tuning LLM on the LongBench dataset here. Table 2 shows the results with 25% KV budgets on Mistral-7B-Instruct-v0.3. We found that to achieve the same level of sparsity, Mistral-7B requires a larger sparse regularization value λ (the value that we used in Table 2 is $1e-6$, which is 10 times larger than the one that we used for Llama3-8B models). The result confirms our conclusion that NAtS outperforms the other baselines in most datasets under similar budget level (and many times with an even smaller budgets).

LLAMA3-8B 50% Budget						Mistral-7B 50% Budget					
	Full	Duo	SLLM	H2O	NAtS		Full	Duo	SLLM	H2O	NAtS
NarrativeQA	27.3	25.1	24.4	25.26	23.95(20%)	NarrativeQA	29.2	26.9	27.3	24.0	28.2 (25%)
Qasper	28.9	27.8	19.8	21.2	28.74 (36%)	Qasper	41.3	35.6	25.1	27.9	39.84 (40%)
MultiFieldQA-en	52.3	50.8	45.6	38.7	50.91 (31%)	MultiFieldQA-en	52.5	52.5	47.0	40.1	52.8 (36%)
MultiFieldQA-zh	50.9	52.64	37.3	37.3	48.13(37%)	MultiFieldQA-zh	58.0	55.4	49.1	39.4	56.26 (32%)
HotpotQA	40.6	42.45	34.0	38.6	40.76(25%)	HotpotQA	49.6	52.94	42.0	47.2	52.1(34%)
2WikiQA	29.3	30.13	25.7	28.1	25.47(27%)	2WikiQA	40.0	39.3	32.8	38.1	39.75 (37%)
Musique	24.4	22.9	21.6	21.6	23.18 (24%)	Musique	28.4	29.45	21.5	20.6	24.3(33%)
DuReader (zh)	30.2	29.84	23.2	23.2	26.41(29%)	DuReader (zh)	34.9	36.44	34.5	26.8	34.42(26%)
GovReport	34.1	32.1	32.2	28.5	33.97 (29%)	GovReport	34.9	32.1	32.6	30.6	33.73 (33%)
QMSum	24.5	24.61	22.8	22.8	23.63(23%)	QMSum	25.7	24.2	22.9	22.5	25.19 (31%)
MultiNews	27.7	27.8	26.3	25.0	27.92 (40%)	MultiNews	27.9	27.0	26.3	25.6	27.32 (47%)
VCSUM (zh)	11.3	7.6	13.03	13.0	8.03(28%)	VCSUM (zh)	16.3	15.6	15.7	15.8	16.04 (24%)
TREC	71.0	73.0	68.0	64.5	69.5(30%)	TREC	75.5	74.5	69.5	66.0	75.0 (42%)
TriviaQA	87.7	86.9	85.0	85.7	87.36 (26%)	TriviaQA	88.9	87.4	88.6	88.4	89.05 (35%)
SAMSum	42.5	41.37	40.6	40.8	41.32(20%)	SAMSum	47.3	44.9	46.1	45.8	46.46 (29%)
LSHT	38.0	31.5	27.2	27.2	37.0 (29%)	LSHT	39.8	37.5	30.0	31.5	40.5 (26%)
Passage Count	1.0	1.0	1.0	1.5	5.14 (30%)	Passage Count	5.5	6.0	3.0	4.0	4.5(34%)
PassageRetrieval-en	80.5	82.5	42.5	68.5	75.05(22%)	PassageRetrieval-en	98.0	99.0	56.0	81.0	94.5(30%)
PassageRetrieval-zh	61.2	61.64	51.5	51.5	45.79(32%)	PassageRetrieval-zh	96.5	96.5	46.5	76.0	87.5(28%)
LCC	37.5	37.1	40.3	41.39	38.3(44%)	LCC	50.7	51.1	49.3	52.23	51.84(50%)
RepoBench-P	38.0	39.4	41.6	40.0	39.72(35%)	RepoBench-P	54.8	53.6	52.3	55.66	54.51(45%)

Table 3. LongBench Results with 50% Budget Size LLama3-8B and Mistral-7B. .

Table 3 shows the evaluation results on LongBench with 50% budgets. Despite having fewer KV cache budgets in all the datasets, NAtS still achieves comparable performance on the LLama3-8B model and better results on the Mistral model and generally performs comparable to the results with the full attention transformers.

D. Ablation Study

D.1. Sparse Regularization Term λ

	Full	NAtS 1e-6	NAtS 5e-7	NAtS 1e-7	NAtS 5e-8	NAtS 1e-8
NarrativeQA	27.3	18.71(3%)	20.79(4%)	23.09(13%)	23.95(20%)	26.11 (49%)
Qasper	28.9	<u>25.55</u> (11%)	28.35 (13%)	29.01 (26%)	28.74 (36%)	28.24 (63%)
MultiFieldQA-en	52.3	38.76(9%)	<u>45.68</u> (12%)	<u>48.72</u> (22%)	50.91 (31%)	53.27 (57%)
MultiFieldQA-zh	50.9	<u>40.55</u> (12%)	<u>45.04</u> (15%)	<u>46.03</u> (27%)	<u>48.13</u> (37%)	46.6(64%)
HotpotQA	40.6	31.71(6%)	<u>34.92</u> (8%)	41.7(17%)	<u>40.76</u> (25%)	<u>40.76</u> (49%)
2WikiQA	29.3	<u>25.9</u> (9%)	<u>26.08</u> (11%)	<u>27.39</u> (20%)	<u>25.47</u> (27%)	<u>27.76</u> (51%)
Musique	24.4	16.25(5%)	<u>19.08</u> (7%)	21.0(16%)	23.18 (24%)	24.0 (48%)
DuReader (zh)	30.2	26.23(7%)	30.0 (9%)	28.44(20%)	26.41(29%)	27.69(57%)
GovReport	34.1	25.52(7%)	<u>29.19</u> (9%)	33.47 (20%)	33.97 (29%)	34.29 (55%)
QMSum	24.5	<u>22.88</u> (5%)	<u>23.24</u> (6%)	<u>23.88</u> (15%)	<u>23.63</u> (23%)	<u>24.18</u> (49%)
MultiNews	27.7	<u>26.83</u> (19%)	<u>27.22</u> (21%)	<u>27.77</u> (32%)	27.92 (40%)	27.97 (65%)
VCSUM (zh)	11.3	12.35(7%)	12.58(9%)	9.4(19%)	8.03(28%)	8.86(58%)
TREC	71.0	57.0(10%)	58.0(11%)	<u>68.5</u> (22%)	<u>69.5</u> (30%)	<u>69.5</u> (56%)
TriviaQA	87.7	84.67(7%)	87.89 (9%)	87.42 (18%)	87.36 (26%)	88.37 (51%)
SAMSum	42.5	<u>41.03</u> (6%)	41.39 (7%)	41.78 (14%)	<u>41.32</u> (20%)	<u>40.91</u> (43%)
LSHT	38.0	23.5(6%)	<u>27.0</u> (8%)	35.5 (20%)	37.0 (29%)	39.5 (58%)
Passage Count	1.0	0.0(8%)	0.5(10%)	1.59 (23%)	5.14 (30%)	2.09 (52%)
PassageRetrieval-en	80.5	12.0(5%)	46.5(7%)	<u>67.0</u> (15%)	<u>75.05</u> (22%)	81.0(47%)
PassageRetrieval-zh	61.2	5.62(10%)	14.88(12%)	<u>41.07</u> (24%)	<u>45.79</u> (32%)	<u>50.34</u> (60%)
LCC	37.5	43.91 (18%)	44.07 (20%)	40.11(35%)	38.3(44%)	38.5(68%)
RepoBench-P	38.0	42.8 (9%)	41.87 (11%)	42.63 (25%)	39.72(35%)	39.18(59%)

Table 4. Ablation Study of Sparse Regularization values λ for LLama3-8B

	Full	NAtS 5e-6	NAtS 1e-6	NAtS 5e-7	NAtS 1e-7	NAtS 5e-8
NarrativeQA	29.2	<u>25.1</u> (3%)	<u>26.84</u> (14%)	28.2 (25%)	28.44 (56%)	<u>26.34</u> (60%)
Qasper	41.3	35.82 (11%)	41.05 (27%)	39.84 (40%)	40.21 (69%)	41.47 (73%)
MultiFieldQA-en	52.5	<u>45.73</u> (9%)	53.07 (24%)	52.8 (36%)	53.17 (64%)	<u>52.31</u> (69%)
MultiFieldQA-zh	58.0	<u>42.81</u> (8%)	55.47 (19%)	56.26 (32%)	56.6 (65%)	56.69 (68%)
HotpotQA	49.6	<u>49.94</u> (7%)	53.02 (22%)	52.1(34%)	50.49(59%)	51.46(63%)
2WikiQA	40.0	<u>35.2</u> (9%)	<u>37.22</u> (25%)	39.75 (37%)	<u>36.57</u> (61%)	<u>36.26</u> (65%)
Musique	28.4	<u>22.5</u> (6%)	<u>26.29</u> (21%)	<u>24.3</u> (33%)	<u>27.33</u> (58%)	<u>26.45</u> (62%)
DuReader (zh)	34.9	32.12(5%)	<u>34.4</u> (15%)	<u>34.42</u> (26%)	<u>34.83</u> (60%)	<u>35.72</u> (62%)
GovReport	34.9	<u>30.38</u> (6%)	33.31 (20%)	33.73 (33%)	34.03 (62%)	34.72 (67%)
QMSum	25.7	<u>23.02</u> (5%)	25.48 (19%)	25.19 (31%)	25.4 (61%)	25.76 (66%)
MultiNews	27.9	27.12 (17%)	27.32 (35%)	27.32 (47%)	27.89 (73%)	27.85 (79%)
VCSUM (zh)	16.3	<u>15.25</u> (5%)	16.21 (13%)	16.04 (24%)	16.1 (57%)	16.57 (61%)
TREC	75.5	69.0(10%)	73.0(29%)	75.0 (42%)	75.0 (66%)	75.5 (71%)
TriviaQA	88.9	<u>87.66</u> (8%)	88.8 (23%)	89.05 (35%)	<u>88.56</u> (61%)	<u>87.14</u> (65%)
SAMSum	47.3	<u>45.42</u> (6%)	<u>45.68</u> (19%)	46.46 (29%)	<u>45.76</u> (52%)	46.19 (61%)
LSHT	39.8	<u>28.25</u> (4%)	39.75 (15%)	40.5 (26%)	40.75 (60%)	38.25 (63%)
Passage Count	5.5	3.5(6%)	4.56(22%)	4.5(34%)	4.56(60%)	5.5(64%)
PassageRetrieval-en	98.0	25.0(6%)	57.5(19%)	<u>94.5</u> (30%)	<u>82.5</u> (56%)	<u>98.0</u> (60%)
PassageRetrieval-zh	96.5	11.5(7%)	<u>58.07</u> (17%)	<u>87.5</u> (28%)	<u>91.5</u> (61%)	<u>95.0</u> (64%)
LCC	50.7	<u>51.42</u> (16%)	<u>51.27</u> (36%)	<u>51.84</u> (50%)	50.17(74%)	50.06(78%)
RepoBench-P	54.8	52.75(10%)	55.98 (30%)	<u>54.51</u> (45%)	<u>54.4</u> (69%)	53.58(72%)

Table 5. Ablation Study of Sparse Regularization values λ for Mistal-7B

We first study the impact of sparse regularization terms. The result is shown in Table 4 and 5. We underline the results that are better than the optimal baselines with 25% budgets, and bold the results that are better than the optimal baselines with 50%. Despite that NAtS in Table 1 ($NAtS\ 1e - 7$) and Table 2 ($NAtS\ 1e - 6$) used more than 25% overall KV budgets for some tasks, here we show $NAtS$ could still outperform many of the corresponding optimal baselines with a even lower KV budget.

Table 4 and 5 show that stronger λ generally results in a smaller valid KV cache size. While the order for compression rates for different datasets is consistent with different λ settings. For most tasks, a compression rate between 10% to 20% already results in predictions that are similar to the full attention.

D.2. Sliding Window Length W

Another important hyperparameter for NATS is the sliding window size W . We apply different sliding window sizes W (64, 128, 256, 384, 512) to fine-tune the Llama3-8B model (with $\lambda = 1e - 7$).

	Full	NAtS 64	NAtS 128	NAtS 256	NAtS 384	NAtS 512
NarrativeQA	27.3	22.94(22%)	24.43(16%)	23.09(13%)	23.64(12%)	24.23(11%)
Qasper	28.9	29.46(32%)	28.13(29%)	29.01(26%)	27.3(27%)	27.29(28%)
MultiFieldQA-en	52.3	48.81(28%)	50.69(25%)	48.72(22%)	48.6(23%)	48.86(24%)
MultiFieldQA-zh	50.9	44.64(30%)	47.79(29%)	46.03(27%)	47.9(28%)	45.71(30%)
HotpotQA	40.6	38.86(25%)	42.78(22%)	41.7(17%)	39.83(16%)	38.82(16%)
2WikiQA	29.3	27.42(27%)	29.9(23%)	27.39(20%)	25.22(20%)	25.31(20%)
Musique	24.4	19.5(25%)	24.48(21%)	21.0(16%)	22.97(15%)	21.16(14%)
DuReader (zh)	30.2	26.82(27%)	26.7(24%)	28.44(20%)	29.7(19%)	30.43(19%)
GovReport	34.1	34.2(28%)	33.45(23%)	33.47(20%)	33.58(19%)	34.18(20%)
QMSum	24.5	23.27(23%)	23.62(17%)	23.88(15%)	24.14(14%)	23.64(15%)
MultiNews	27.7	27.58(32%)	27.69(32%)	27.77(32%)	27.74(35%)	27.74(39%)
VCSUM (zh)	11.3	6.73(26%)	7.38(21%)	9.4(19%)	8.49(19%)	10.17(20%)
TREC	71.0	69.0(31%)	70.0(26%)	68.5(22%)	72.0(21%)	70.0(22%)
TriviaQA	87.7	85.79(26%)	86.92(23%)	87.42(18%)	87.28(18%)	88.23(18%)
SAMSum	42.5	41.76(24%)	41.46(18%)	41.78(14%)	41.48(14%)	42.18(15%)
LSHT	38.0	32.0(27%)	38.0(24%)	35.5(20%)	33.5(19%)	36.5(19%)
Passage Count	1.0	2.55(27%)	4.09(26%)	1.59(23%)	0.5(22%)	1.05(22%)
PassageRetrieval-en	80.5	59.0(25%)	69.5(20%)	67.0(15%)	65.5(14%)	61.0(14%)
PassageRetrieval-zh	61.2	38.45(29%)	42.8(26%)	41.07(24%)	36.49(24%)	42.47(25%)
LCC	37.5	43.3(34%)	40.2(37%)	40.11(35%)	41.28(36%)	44.08(40%)
RepoBench-P	38.0	44.02(31%)	42.63(31%)	42.63(25%)	42.94(23%)	42.76(23%)

Table 6. Ablation Study of Sliding Window Length W for Llama3

The result is shown in Table 6. Overall, all the approaches performs similarly. However, smaller sliding window size generally results in an overall larger KV cache size. A reduced sliding window size would force the model to apply more Global Tokens and Local Tokens to construct the mid-range correlation since this distance cannot be covered by the sliding window tokens. However, as the number of sliding window size further increases, this compression rate might saturate since the remaining tokens might always require a long-range correlation whose distance is much larger than the sliding window size (e.g., these tokens might require the correlation between two tokens whose distances are larger than 1k or even more).

E. Further Results on KV size distributions

Figure 7 shows the KV cache sizes for LLama3-8B and Mistral-7B on the MultiNews Dataset. The two models still share some similar structure: both modules assign more budgets to the first few layers. However, the KV cache sizes are more uniformly distributed in Mistra compared to LLama3: in LLama3, most of the time, one or two heads with a much larger KV cache sizes compared to the other heads in the same layer, while in Mistral models, this is not so obvious.

Figure 8 shows another example on the DuReader dataset. This time, we check two other cases: one with a relatively lowered KV cache size, as shown in the upper part of Figure 8. The KV cache sizes are further sparsely distributed even in the shallower layers. However, the important layers in different models are not fixed: in LLama3, 9 layers (1, 3, 5, 6, 9, 11, 15, 16, 17) require a relatively larger budget while this value is much smaller for Mistral: only layer 3, 8, 13, 16 and 19 requires a relatively larger KV cache size. This further shows the importance of designing data and model adaptive approach for compressing the KV cache optimization policies.

Neural Attention Search



Figure 7. KV size of LLama and Mistral on MultiNews Dataset

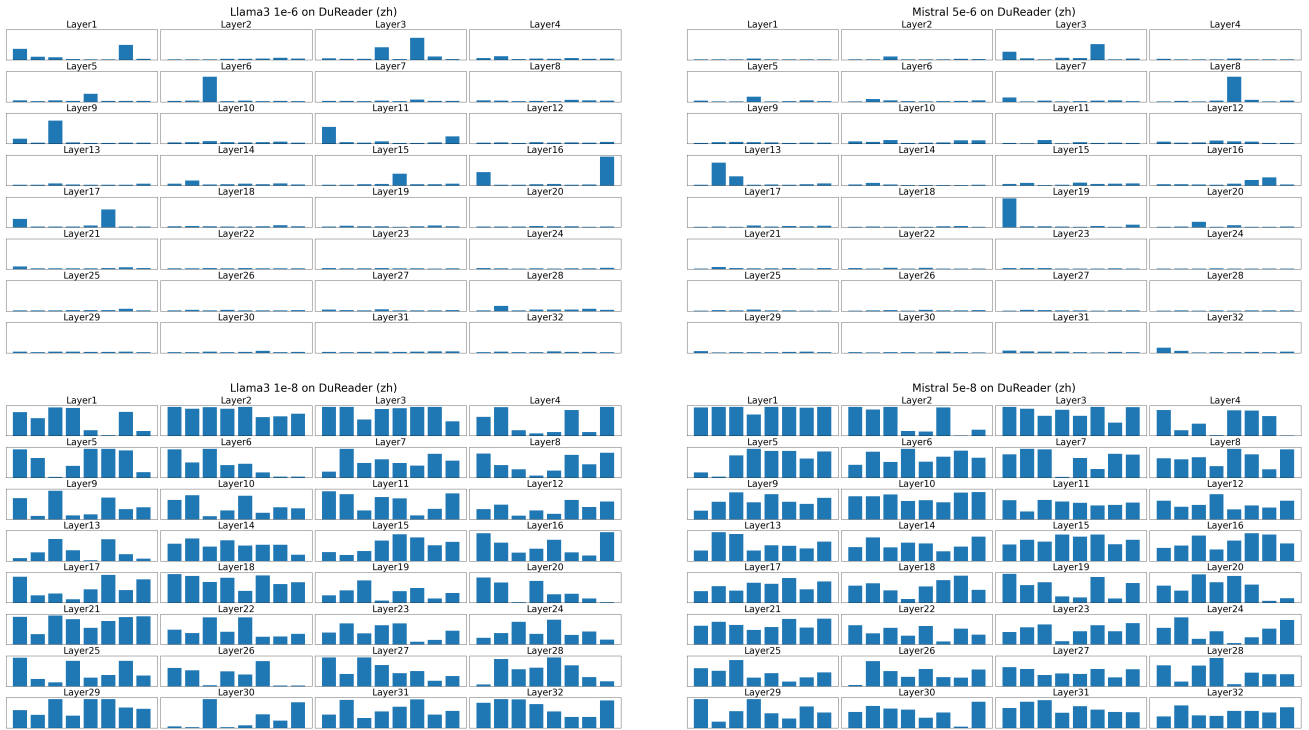


Figure 8. KV size of LLama and Mistral on DuReader Dataset